MODEL QUALIFICATION OF TEST CAVERNS ON FIELD TEST DATA

HYPSTER PROJECT

Deliverable 2.6

Authors: M. Glöckner (ESK), M. Schlichtenmayer (ESK), A. Bannach (ESK), G. Hevin (Storengy)

Project acronym:	**HyPSTER**
Project full title:	Hydrogen Pilot Storage for large Ecosystem Replication
Grant Agreement No. :	101006751
Duration :	36 months
Start date :	1st January 2021
2020 AWP topic addressed:	Topic 2.7 – Cyclic testing of renewable hydrogen storage in a small salt cavern
Coordinator's contact details:	Jean-François Guerin jean-francois.guerin@storengy.com

Version #	Implemented by	Revision date	Changes
V1	M. Schlichtenmayer	19.09.2024	First draft
V2	M. Glöckner	15.08.2025	Draft model validation
V3	M. Schlichtenmayer	19.09.2025	Final version

Submission date: 19.09.2025
Status: Final

Co-funded by the European Union

Clean Hydrogen Partnership

"This project has received funding from the Fuel Cells and Hydrogen 2 Joint Undertaking (now Clean Hydrogen Partnership) under Grant Agreement No 101006751. This Joint Undertaking receives support from the European Union's Horizon 2020 Research and Innovation programme, Hydrogen Europe and Hydrogen Europe Research."

Table of content

1. INTRODUCTION

The HyPSTER project is the first EU-funded demonstrator for hydrogen storage in salt caverns. In addition to preparing the demonstration of storing hydrogen in salt caverns at the site Étrez, France, the project is also meant to facilitate the replication of the technology in other locations around Europe.
Therefore, a small cavern (EZ 53) was selected for experimental purposes. The cavern EZ 53 had been subject to several investigations in the past like Hugout test and outflow tests ([1], [2], see also deliverable D2.4).
Within the HyPSTER project, this cavern has been subject to further investigations. After the installation of a hydrogen-proof well completion, the cavern and equipment had passed several tightness tests (nitrogen, hydrogen). As the cavern and completion have successfully passed the tightness tests an amount of approximately 2.6 t of pure hydrogen were injected replacing the brine in the upper section of the cavern. A major part of the cavern remained filled with brine. Afterwards, starting in December 2024 cyclic tests with hydrogen have been performed in the upper part of the cavern EZ 53 by injection / withdrawal of brine into the cavern to increase / decrease the hydrogen pressure in the upper part of the cavern.
These cyclic tests are evaluated in this report using the software model (KAVPOOL), which was already tested earlier in the project (see deliverable D2.1). By successfully matching the measured data with the modeling, this model is qualified for further field application.

2. SUMMARY OF EZ53 CHARACTERISTICS

At the Storengy site of Etrez, the EZ53 is a relatively small cavern formed through solution mining in the spring of 1982. However, due to evolving conditions in the gas market, the decision was made to stop the leaching process prematurely—before the cavern could develop into its originally intended final dimensions. Consequently, EZ53 features a tall, narrow chimney structure extending from 846 m to 920 m in depth, and its total volume remains limited.
A recent sonar survey carried out in 2023, measured the cavern's volume to be approximately 7,381 cubic meters (Figure 1, left).
The upper salt layer at the Etrez site contains a significant proportion of insoluble material, about 5 to 10% mainly composed of clay and thin anhydrite seams. One such layer, clearly identifiable at a depth of 928–930 meters, separates a small void from the main cavern body [2]. This small void is referred to here as the "upper cavern" and has a volume of approximately 230 m³ (280 m³ including the narrow connection to the “lower cavern”).
The cyclic tests have used the upper cavern as the space for hydrogen. The majority of the cavern EZ 53 was therefore filled with brine (Figure 1, left). Injection or withdrawal of brine through the installed debrining string (4,5 inch) leads to compression or expansion of the hydrogen in the upper cavern and corresponding changes in pressure and temperature. The amount of brine in the debrining string until the H2-brine interface accounts for about 7,7 m³. The annular space to the top of the upper cavern filled with hydrogen in the tests yields about 12,6 m³.

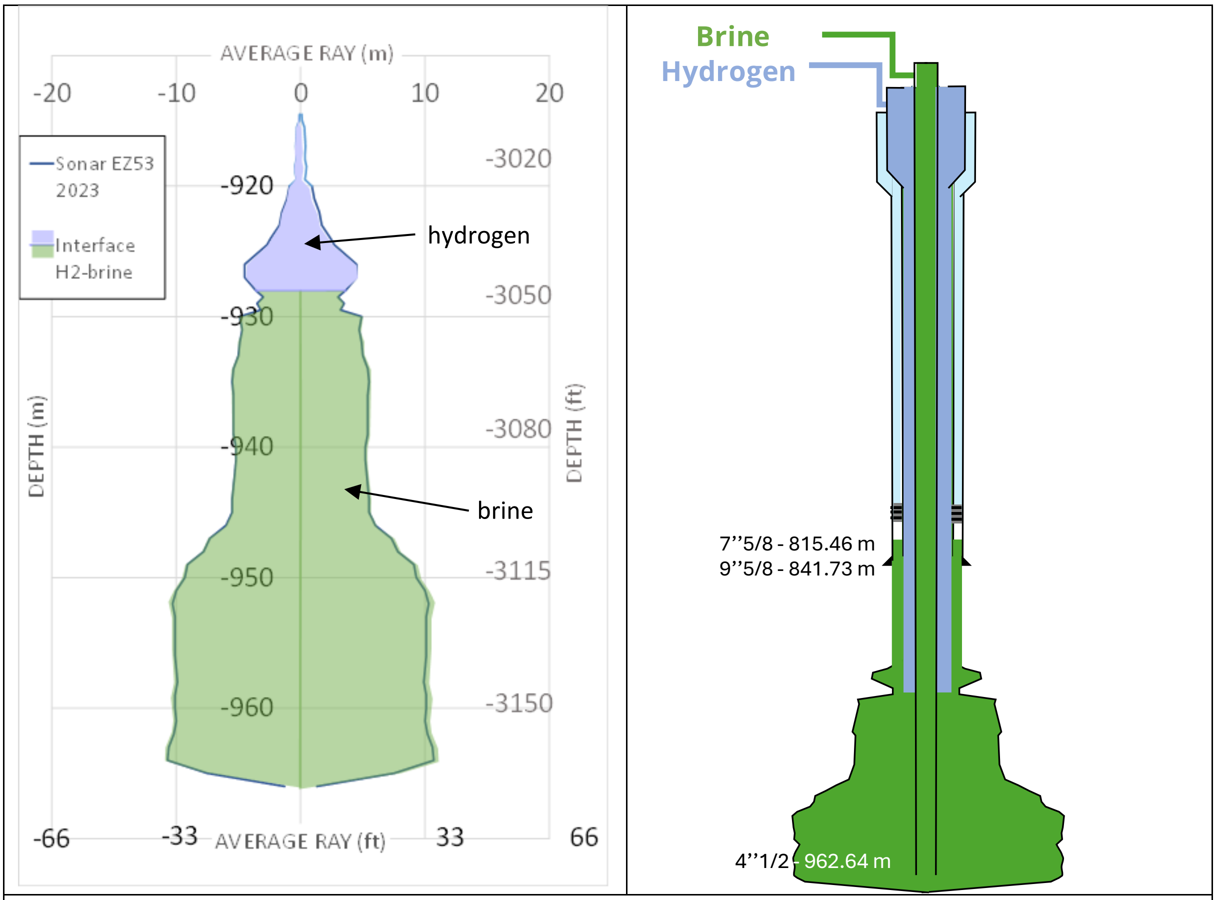

Figure 1. EZ53 sonar survey in 2023 with content of cyclic test (WP3) (left), EZ53 completion [2] (right)

3. APPLIED SOFTWARE MODEL

The used software suite KAVPOOL is focused on the modeling of thermodynamical effects in the cavern, the well and the surrounding rock and the coupled operation of multiple caverns in a storage pool. It also includes a cavern convergency module that can be coupled with the commercial software FLAC3D to allow detailed geomechanical modeling. The modeling algorithm is based on the laws of mass and energy conservation, classical heat conduction within rock mass (Fourier's law), heat transfer between gas, solid and liquid (sump) by heat transfer coefficients, different flow regimes including choked flow and gas mixtures with up to 12 typical gas components (Redlich-Kwong approach).

Benchmark tests were conducted beforehand using two software models, the KAVPOOL suite and LOCAS (2D-FEM). A sensitivity analysis was conducted on 19 cases considering five yearly-cycles (see deliverable D2.1). In general, the pressure difference between both models was in the order of less than 1 bar, which is considered acceptable. Larger differences of the model results could be observed at operating conditions beyond the normal operating range range, e.g. at flow velocities above 100 m/s or for deep caverns in fast creeping rock salt.

Based on the calculations performed and the comparative analysis of the calculation results generated, it can be concluded that the calculation models investigated appear suitable to the modelling of the cycling tests and for future applications in association with the storage of hydrogen in solution-mined salt caverns.

4. PREDICTIVE MODELING OF EZ53 CYCLIC TEST

A proposal for the Cyclic Test Program was prepared from within Task 2.1, which combines the general requirements on the test (mainly operational aspects and the need to perform a minimum of 100) with scientific aspects (to facilitate the validation of the software models with the test data). This proposed program consists of a superposition of large-scale cycles with a duration of multiple days and small-scale cycles with a duration of some hours. It also has several standstill periods, which should allow an improved model calibration. If technically possible, a final hydrogen release should be performed at the end of the cyclic testing to include the low-pressure range in the test, which is not possible in the cycling mode with brine compensation operations.

The schedule below includes several standstill periods for improved model calibration and more than 100 intraday cycles. The last pressure decrease reaches smaller pressures than before, because here the fluid in the central string can be technically replaced by fresh water instead of brine allowing a larger pressure difference between well head and cavern. Afterwards, a final withdrawal of the hydrogen (red line after day 100) would allow taking additional data for model calibration. The proposed test schedule is described in detail in the deliverable D2.2.

The complete test cycle for predictive modeling is illustrated in **Fehler! Verweisquelle konnte nicht gefunden werden.**.

The planned cyclic test have been modelled thermodynamically with KAVPOOL. This model was initialized with the parameter set specified in Table 1.

Table 1: Summary of initial parameters for thermodynamical modelling of EZ53 cyclic tests

Property	Unit	Value
Depth of last cemented casing shoe	m	842
Depth of tubing shoe	m	929
Depth of cavern roof	m	920
Depth of cavern sump	m	929
Depth of salt top	m	690
Casing dimension	-	9 5/8”, 40 lbs/ft
Tubing dimension	-	7 5/8”, 29.7 lbs/ft
Debrining string dimension	-	4 ½", 10.5 lbs/ft
Surface roughness	mm	0,05
Cavern volume (gas-filled)	m^3	245
Total cavern volume	m^3	7381
Effective cavern compressibility	1/MPa	0.00039
Heat transfer coefficient	$W/K/m^2$	30
Heat conductivity of salt rock	W/K/m	6
Specific heat capacity of salt rock	kJ/kg/K	1.0
Density of salt rock	kg/m^3	2200
Surface temperature	°C	11
Rock temperature at cavern center	°C	44.6

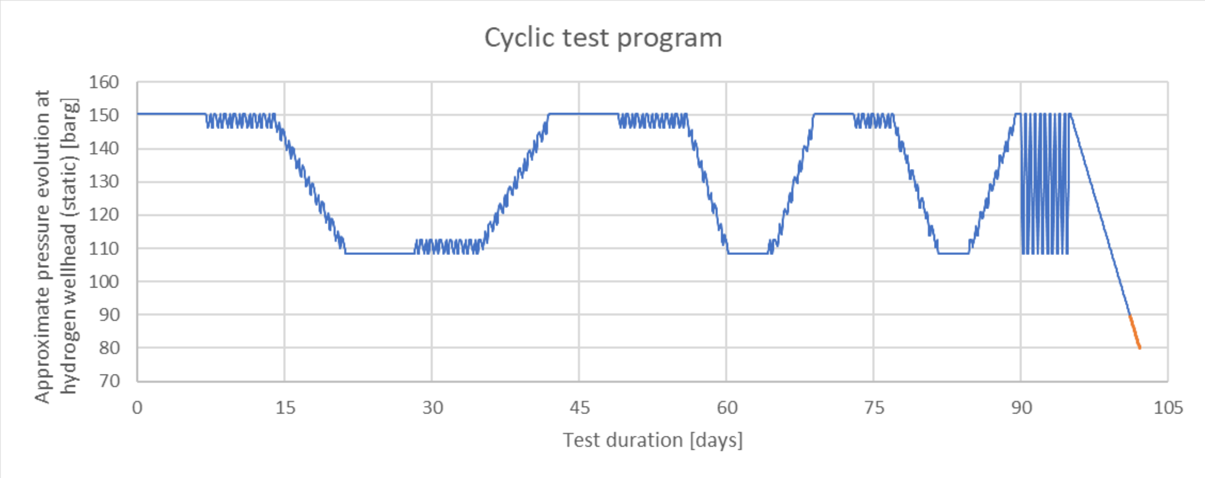

Figure 2: Proposed operating schedule for the cycling test at cavern EZ53

In the modelling, the amount of hydrogen in the cavern is kept constant and, as planned for the conduction of the cyclic tests, the spatial volume filled with hydrogen and, correspondingly, the hydrogen pressure are changed by the injection and withdrawal of brine. The resulting pressure development can be compared with the measured well head pressures. The temperature development is also a result of the modelling, but cannot be measured directly in the installed test setup. Nevertheless, the temperature development is checked for plausibility.

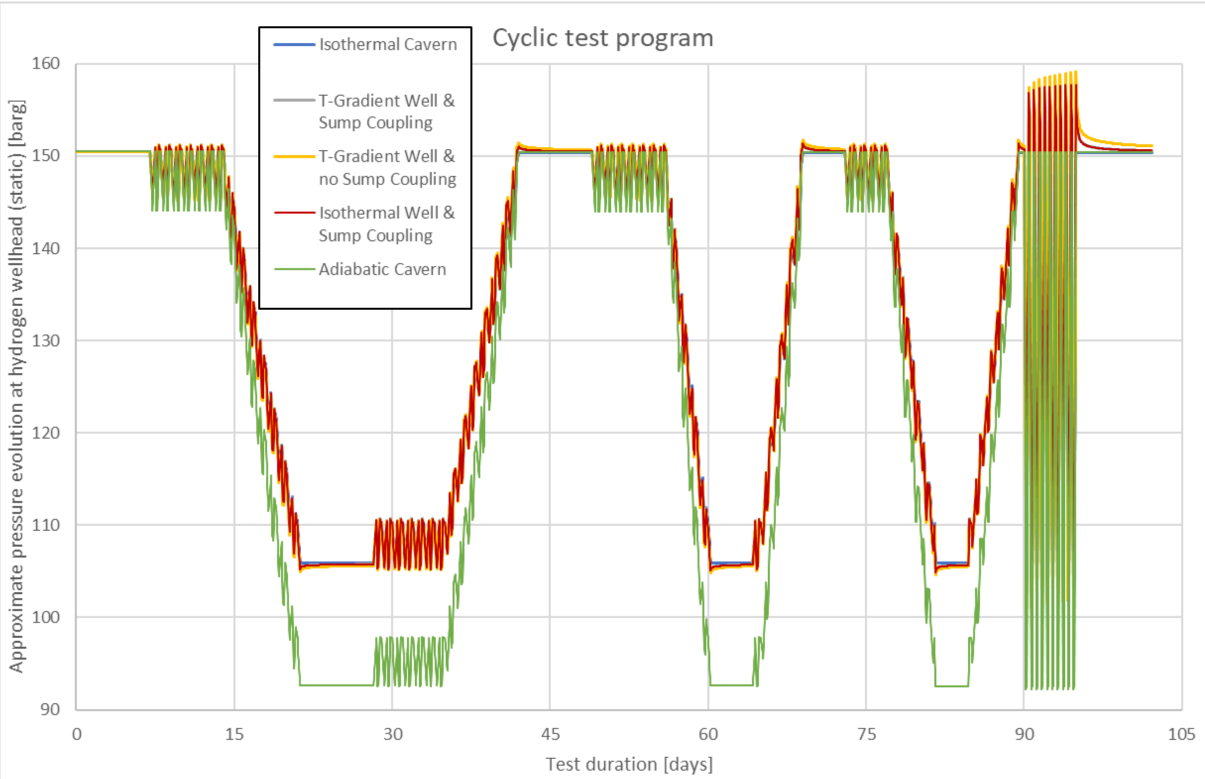

Figure 3: Pressure evolution during predictive thermodynamical modelling of EZ53 cyclic test with a fixed brine rate schedule and different thermal boundary conditions (full range)

During the tests in EZ53 the stored hydrogen is in thermal contact with a very large amount of brine in the cavern sump, much more than in usual storage operations. It is not fully understood how efficient heat can be transferred between the stored gas and the brine, because the flow field of the brine will have a strong impact on this aspect. In the modelling different approaches are applied to capture the potential range of thermal coupling. The most extreme cases are either neglecting the thermal coupling with the sump or assuming thermal equilibrium with the sump (Figure 3Figure 4).

Furthermore, different methods for modelling the temperature distribution in the well have been applied, assuming either linear temperature gradients in the well sections in the salt rock and overburden as boundary conditions or an isothermal well to reflect hydrogen temperatures in the well dominated by the temperature of re-injected brine.

As reference cases, isothermal and adiabatic cavern models have also been included to allow a comparison of different heat transfer efficiencies. In usual natural gas storage operation, the heat transfer coefficient is not predefined or measured directly, but must be determined within a reasonable range by fitting the measured and modelled pressure development (common values are in the range from 10 W/m²/K to 30 W/m²/K). A heat transfer coefficient of 0 W/m²/K would correspond to an adiabatic cavern, while for very large values (over 1000 W/m²/K) thermal equilibrium between the storage inventory and the cavern wall is approached.

The predictive modelling of the planned cyclic tests at EZ53 shows that for the given configuration (very small cavern) the thermal coupling of the storage inventory and its surrounding can have a strong impact on the pressure evolution at a fixed brine rate schedule, when comparing the adiabatic case with the other cases (up to 15 bar pressure difference). However, the more realistic cases are very similar to each other (Figure 3).

Only during the periods with large cycles (Figure 4Figure 3, day 90-95), a pressure difference in the order of up to 5 bar between the isothermal cavern and the more realistic cases can be observed.

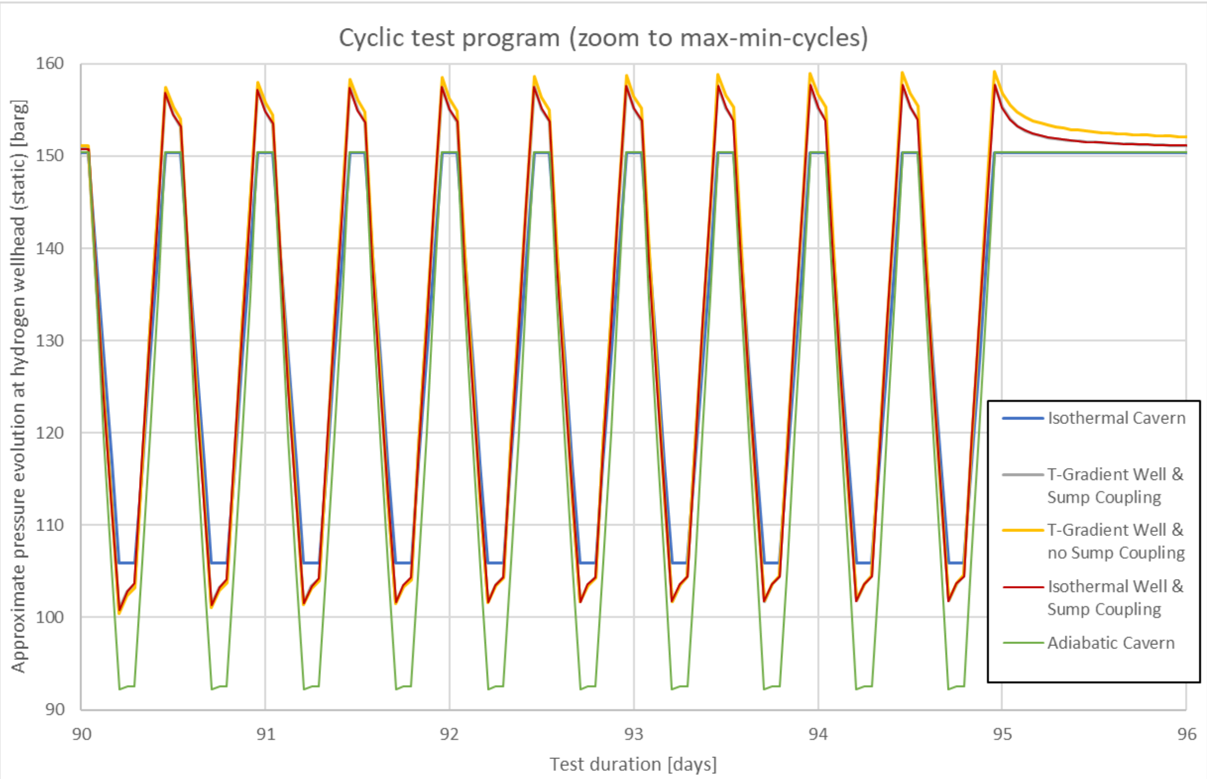

Figure 4: Pressure evolution during predictive thermodynamical modelling of EZ53 cyclic test with a fixed brine rate schedule and different thermal boundary conditions (large cycles)

During the periods with smaller cycles (Figure 5), the pressure difference between all cases (except for the adiabatic case) is very similar. This indicates that the thermal coupling of rock and storage inventory is strong enough during these periods that any heat flux across the cavern wall can be quickly absorbed by the surrounding rock mass.

This observation has a consequence for the fitting of modelled pressure developments to measurement data, because increasing the thermal coupling should have a weak effect to improve the match between model and measurement, only decreasing the thermal coupling should have a relevant effect.

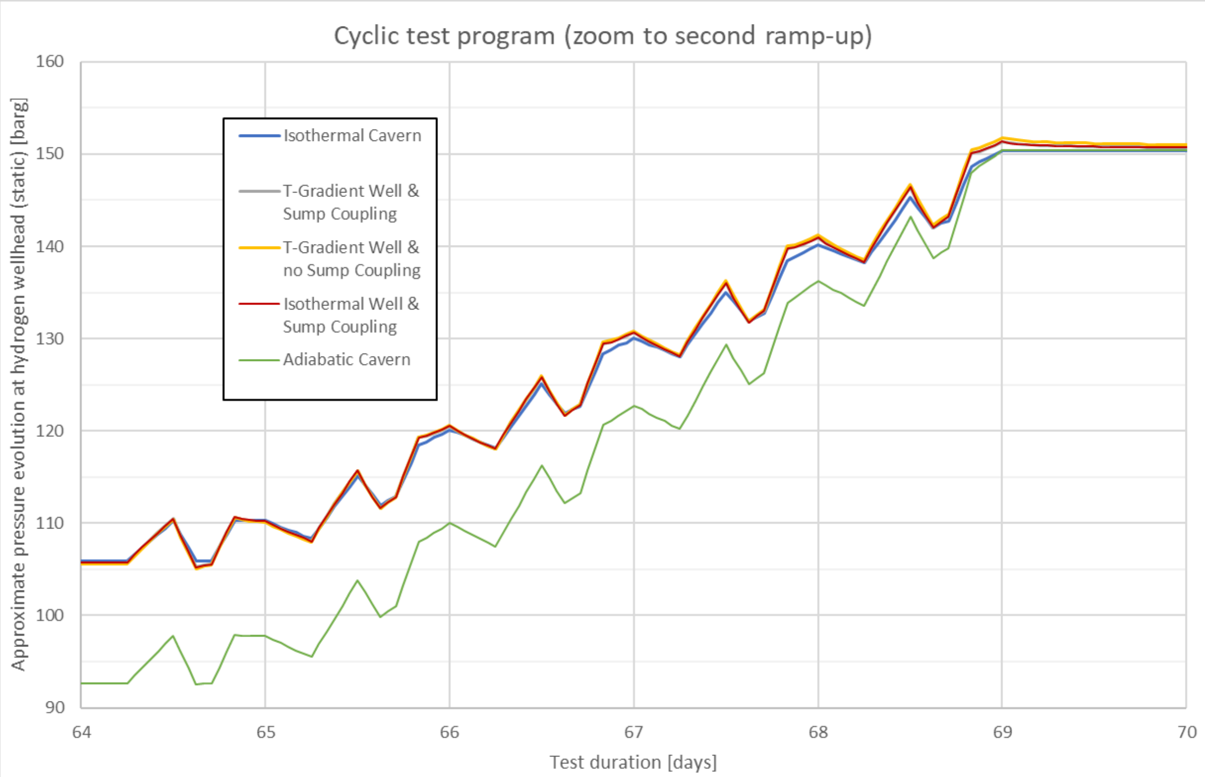

Figure 5: Pressure evolution during predictive thermodynamical modelling of EZ53 cyclic test with a fixed brine rate schedule and different thermal boundary conditions (small cycle ramping up)

5. SUMMARY OF TEST RESULTS

As part of the HyPSTER project, a comprehensive series of cyclic hydrogen storage tests was conducted in the EZ53 salt cavern between November 2024 and May 2025. The test campaign aimed to evaluate the operational behavior of hydrogen under cyclic pressure conditions and to generate high-resolution data for model calibration. A total of 2.6 tons of green hydrogen were injected into the upper part of the cavern, supplied via five tube trailers. The hydrogen inventory remained constant throughout the tests, while pressure modulation was achieved by injecting and withdrawing brine using a reciprocating pump system.

Over 100 pressure cycles were performed, including both small and large amplitude variations (Figure 6). These cycles revealed characteristic thermal effects, such as pressure drift during standstill periods—pressure decreases at high hydrogen levels and increases at low levels—consistent with known behaviors in natural gas storage operations. Technical challenges, including pump-induced vibrations, freezing temperatures, and brine system malfunctions, were encountered but successfully mitigated. Notably, no issues were reported on the hydrogen side of the demonstrator, confirming the robustness of the gas-handling infrastructure.

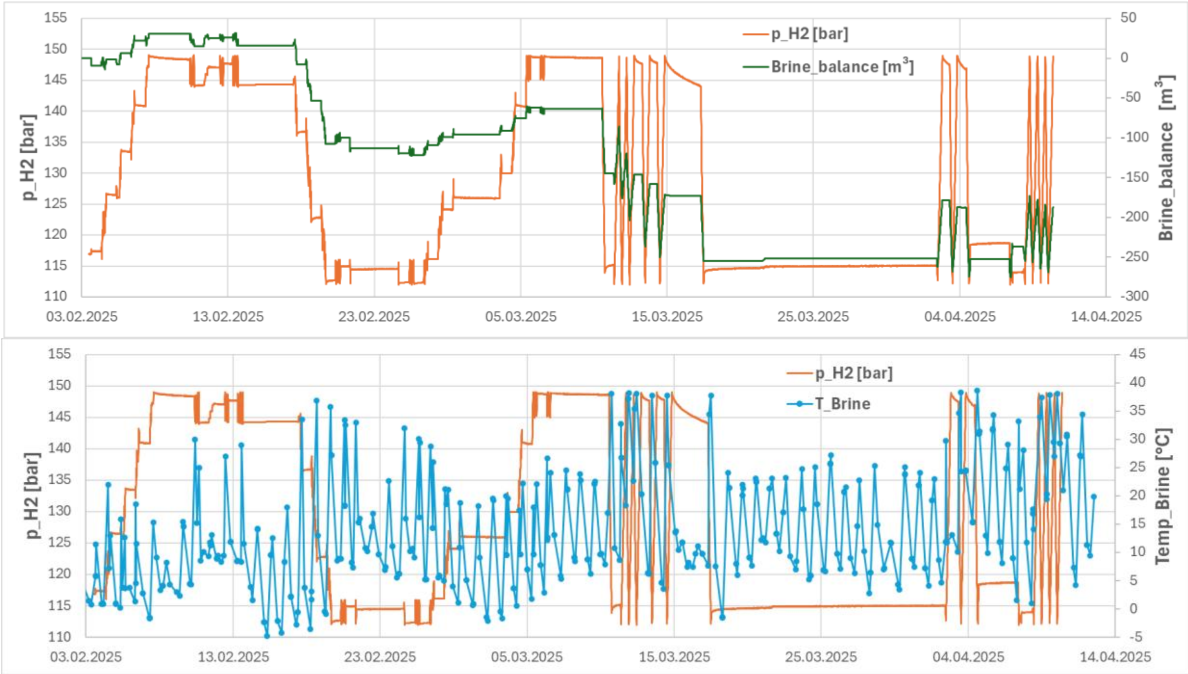

Figure 6: EZ 53 storage platform – All cycles in 2025 showing head pressure (H2), brine balance and temperature

Following the cyclic tests, a two-stage hydrogen withdrawal and full rebrining of the cavern were carried out in May 2025. The venting process was carefully managed to ensure safety and operational control, with hydrogen pressure reduced to as low as 5 bar to enable sampling. The final rebrining restored the cavern to its original state, with no incidents reported.

The data collected throughout this campaign—covering pressure dynamics, thermal behavior, and operational responses—provide a valuable foundation for validating thermodynamic models and designing future hydrogen storage caverns. The following evaluations are mainly based on the measured hydrogen and brine well head pressures, the brine rate and the brine temperature at the wellhead. Furthermore, the temperature measured at the wellhead in the hydrogen connection is used for reference, but as this part of the hydrogen line is separated from the hydrogen in the well by a valve, which was closed during most of the test, this temperature corresponds rather to the surface temperature.

It should also be noted that the evaluation of the test data suffers from the fact that the recorded sampling intervals vary during the test duration and are not identical for all measured quantities. This is particularly relevant for the brine rate, because it is not always clear if the recorded brine rates are valid for the complete time interval, and in some instances the pressure development indicates changes in the brine rate during the corresponding time interval. In the following evaluation, different compensation approaches are described.

6. MODEL VALIDATION

During the conduction of the cyclic test, it turned out that the idealized schedule could not be fully realized as proposed due to various unforeseen technical circumstances. Nevertheless, the main requirements regarding the number of cycles and the operating pressure range were met, and the realized test schedule contains the same qualitative features as the proposed schedule with periods of large-scale cycles, superpositions of large and small-scale cycles and standstill periods in-between. The evaluation focuses on the large cycles (conducted from 10.03.2025 to 10.04.2025), because these offer the best chance to distinguish different thermal effects.

The measured hydrogen and brine wellhead pressures as well as the corrected brine balance during this period is illustrated in Figure 7.

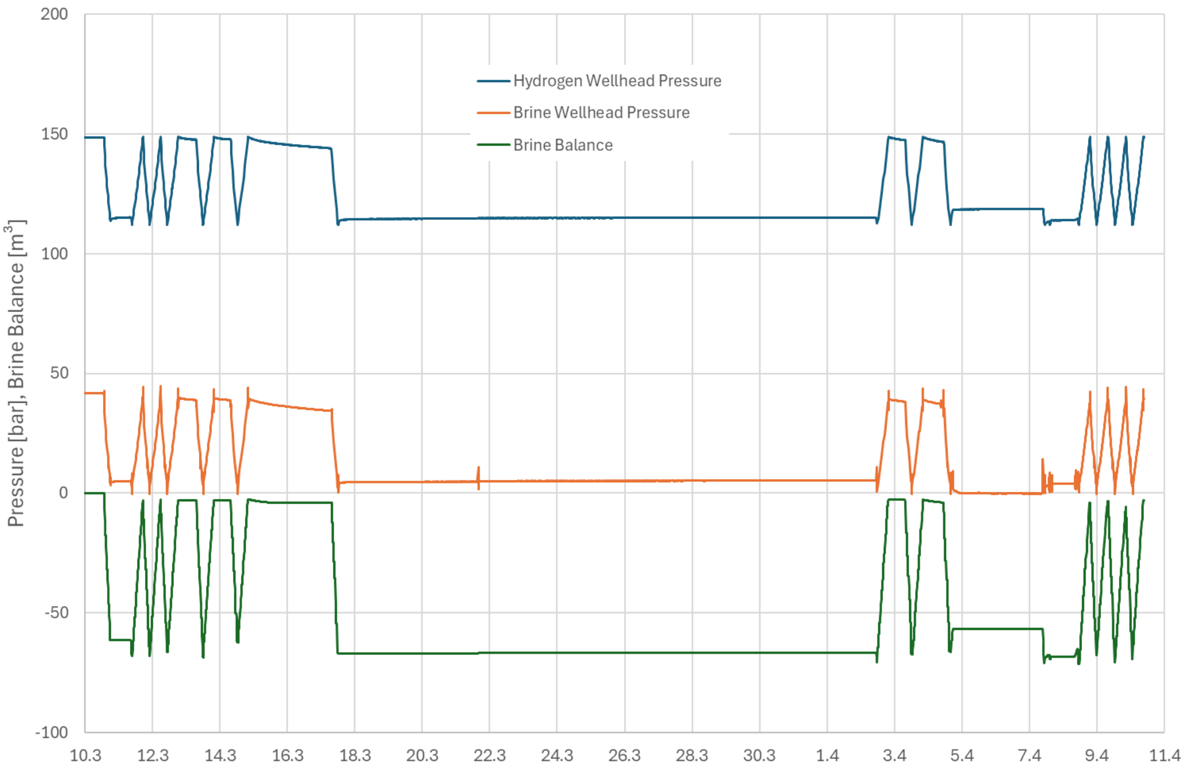

Figure 7: Pressure measurements and corrected brine balance during the large-scale cycles of the EZ53 cyclic test

The brine balance was calculated from the measured brine flow rate including a correction offset for the dilution of the produced brine with fresh water (or low saturated brine), which was necessary to avoid recrystallization in the aboveground piping due to temperature changes. Furthermore, a correction factor was applied to account for the compressibility of the large brine-filled cavern.
In detail, the following steps have been taken to obtain the corrected brine balance:

- Identification of operating mode: as only absolute values are recorded for the brine rate, for each time interval it was identified by the direction of the pressure change whether the cavern was in injection or withdrawal mode. Furthermore, periods with flow rates below 1 m³/h were interpreted as standstill periods.
- Assigning of time intervals: as a simple and robust approach each brine rate recording was assigned to the time interval starting at the midpoint between its own corresponding time stamp and its predecessor and ending at the midpoint between its own time stamp and the following time stamp.
- Accounting for system compressibility: as the total cavern is much larger than the hydrogen volume, the compressibility of the system cannot be neglected. From previous tests a system compressibility coefficient of $\beta = 3.9 \times 10^{-4}/\mathrm{MPa}$ was derived (see also deliverable D2.4). This results in a simplified correction factor of 0.879 to be applied to all recorded brine rate values.
- Correction of freshwater injection: during brine withdrawal fresh water was added to the brine and measured by the flowmeter resulting in larger flow readings. Unfortunately, the freshwater rate was not recorded separately. It can be estimated that the freshwater rate is in the order of a few percent of the brine rate. In practice, an individual scaling factor was applied to each brine withdrawal process to ensure cavern brine balance conservation during each full operating cycle. This scaling factor was in the

order of 0.95 to 1.0 corresponding to freshwater rates less than 1.5 m³/h, or freshwater fractions of less than 5% of the recorded brine rates.

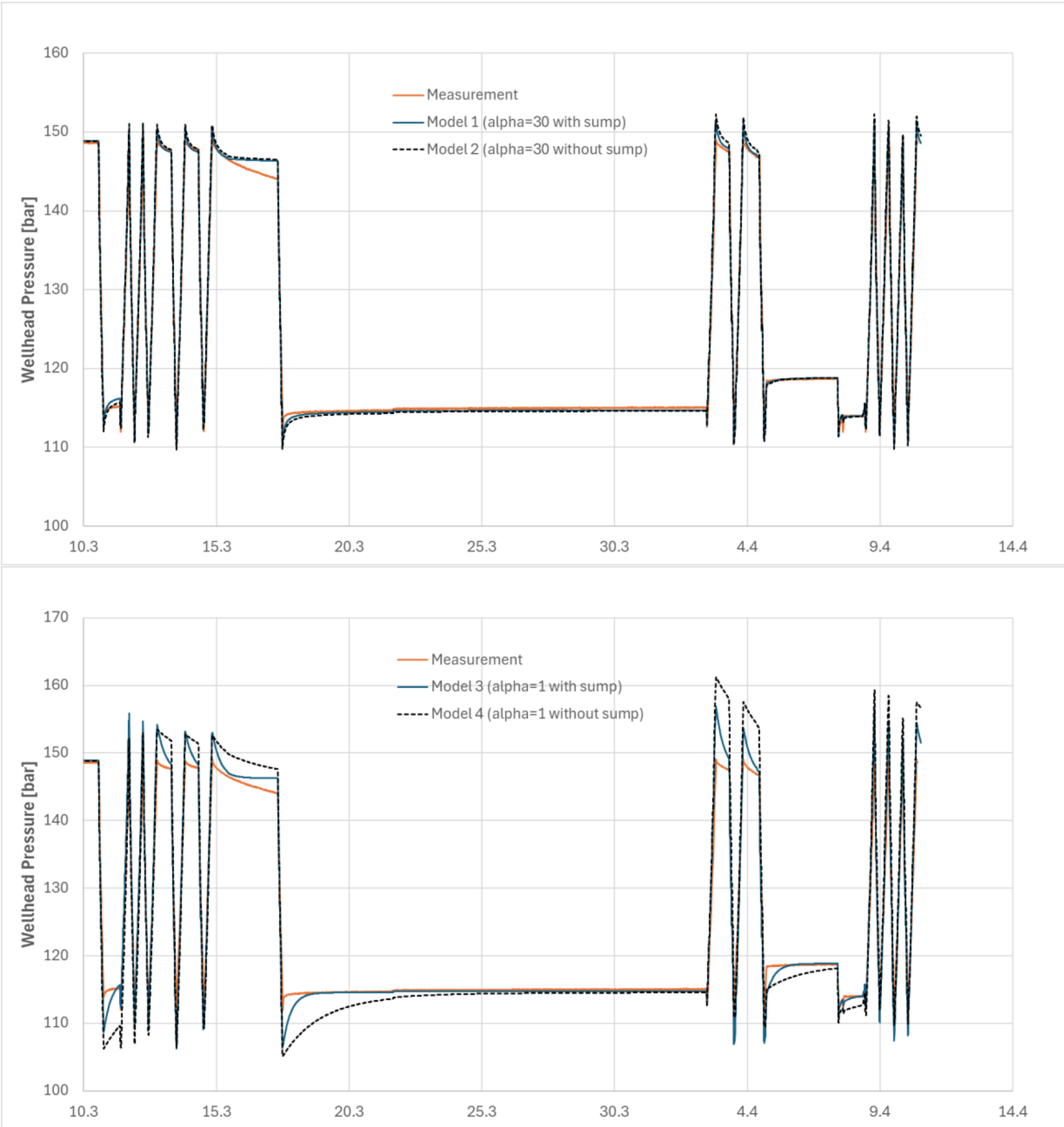

Figure 8: Comparison of measured and modelled wellhead pressure development during the EZ53 large-cycle tests for four exemplary thermal boundary conditions

For the modelling of the actual cyclic test the KAVPOOL model was initialized with the data already used for the predictive modelling (Model 1, see Table 1). Furthermore, as the thermal coupling of the hydrogen inventory and the surrounding rock and brine was identified as major impact factors for the pressure development, variations of the heat transfer coefficient and the sump coupling were included (Model 2: no sump coupling, Model 3: heat transfer coefficient of 1 W/m²/K and sump coupling, Model 4: heat transfer coefficient of 1 W/m²/K without sump coupling). Afterwards the corrected brine rates corresponding to the brine balance shown in Figure 7 were applied and the resulting pressure development was modelled. The modelling results are illustrated in Figure 8 (Model 1 – 4). The comparison of the modelled data with the measurement shows a good agreement for Model

1, as the difference between both is smaller than 2 bar, which is usually considered acceptable. Model 2 uses the same parameters as Model 1 except that the thermal coupling with the sump is neglected. This turns out that including the sump as a heat reservoir has a positive effect on the match between measurement and modelling result.

For comparison two other model initializations with a lower heat transfer coefficient of 1 W/m²/K were applied, while all other parameters remained unchanged relative to the first two models (Model 3 and Model 4, Figure 8, lower panel). The influence of the heat transfer coefficient can be seen, since the match of Model 3 and Model 4 are poorer than the first two models.
Even though Model 4 generally shows a lower agreement with the measurement than the other models, it is interesting to note that the pressure development during the standstill periods at high pressure is almost parallel to the measurement. On the other hand, all other models show a stronger pressure decrease at the beginning of the standstill periods approaching thermal equilibrium after several hours.
It is also observed that during the long standstill period at low pressure from the 17th of March until the 2nd of April, Model 3 and 4 need several days to reach thermal equilibrium, while the measurement and Model 1 and 2 reach thermal equilibrium after less than one day.
Therefore, tuning the thermal coupling in the models leads to a trade-off between matching the pressure measurements during standstill periods either at higher or lower pressure levels.

With a maximum difference in the order of 2 bar between Model 1 and the measured wellhead pressure development, the accuracy of this model can generally be considered acceptable. Nevertheless, additional effort has been taken to further improve the match focusing on three aspects: thermal coupling of hydrogen inventory to the surrounding, standstill periods at high pressure and additional corrections of the brine rate due to its heterogenous sampling intervals.

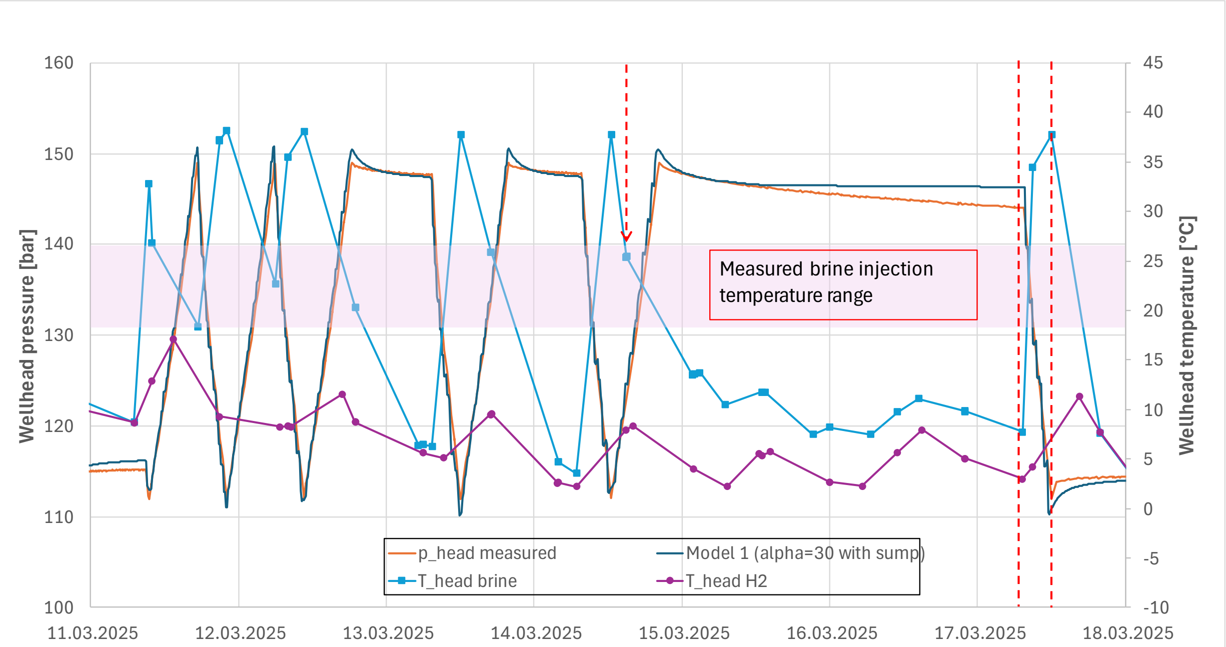

Figure 9: Detailed temperature and pressure development including standstill period from 14th until 17th of March. The red arrow indicates the temperature measurement during brine injection. The following brine withdrawal period is also indicated by red dotted lines. It can be assumed that the temperature measured in the hydrogen at the wellhead corresponds to the ambient temperature at the surface

Thermal coupling

It is very likely that heat can be efficiently transferred from the sump to the hydrogen inventory, when the hydrogen is colder than the brine in the sump (i.e. during standstill periods at low pressure), because the natural thermal convection in the brine will be enhanced, when the heat sink at its top boundary gets colder. Thus, there will be a constant flow of relatively warm brine from the lower levels of the cavern that can transfer heat to the stored hydrogen.

It is complex to assess whether this process will remain effective, when the hydrogen gets warmer than the brine (i.e. during standstill at high pressure). The continuous pressure decrease from 14.03. in the evening until 17.03. in the morning (where pressure was high and, thus, the hydrogen temperature must have been above its surrounding temperature) could be interpreted in the way that the stored hydrogen is still approaching thermal equilibrium during this period, which would indicate a low heat transfer. Figure 9 shows the measured brine temperature during this period. The only temperature measurement during the previous brine injection (25.4 °C) is indicated by a red arrow. As the injected brine is taken from a big container on the surface, it can be assumed that the temperature distribution of this brine is homogenous.

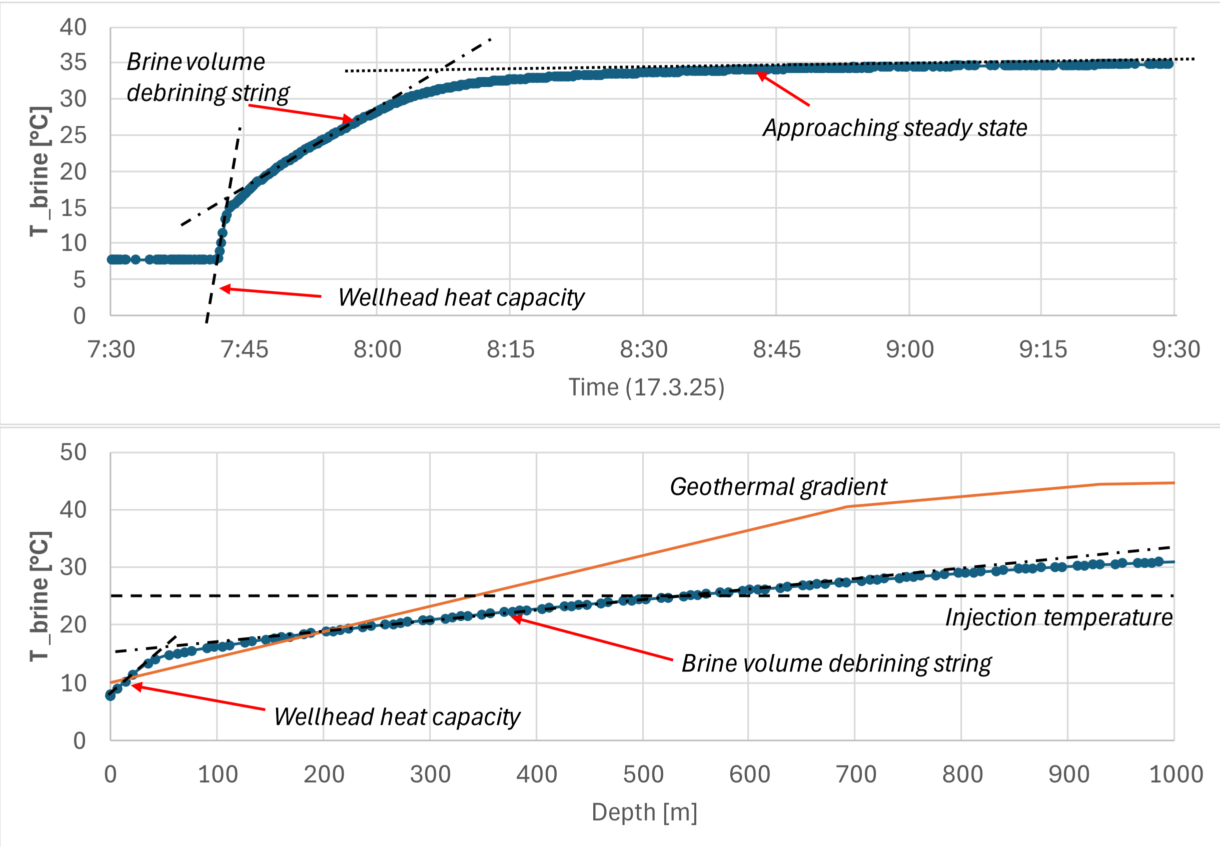

Figure 10 : Detailed temperature measurement during brine withdrawal on the 17th of March

For the brine withdrawal on 17.03. a detailed temperature measurement is available, which is illustrated in Figure 10. A comparison with the measured brine rate reveals that the brine volume, that rested in the central string during standstill, must have been completely withdrawn at 8:05 o'clock. Thus, approximately half of the brine volume from the central string had a temperature below the previous injection temperature of 25.4 °C, and the other half had a higher temperature. Notably, the cavern temperature of 44.6 °C, which was measured during the sonar survey in 2024, was not reached during brine withdrawal, even though a large amount of brine from the lower part of the cavern was produced. This shows that the produced brine loses a significant amount of heat to the surrounding rock along the well. However, the smooth transition of the temperature of brine from the

central string above the hydrogen-brine interface to the temperature of the brine from the deeper cavern gives an indication that there is no significant temperature difference between the brine in the sump and the hydrogen stored above. In contrast, if the hydrogen temperature would still be higher than the brine temperature at the start of the brine withdrawal, this should either be visible in the brine temperature profile, or at least there should be a stronger kink. This gives an indication that the hydrogen is in thermal equilibrium with its surrounding at the end of the standstill period or has at least reached a steady state, which would also exclude the models 3 and 4 in Figure 8 with a heat transfer coefficient of 1 W/m²/K.
Therefore, even if a low heat transition coefficient like 1 W/m²/K would improve the pressure match of model and measurement during the high-pressure standstill periods, this approach is not supported by the temperature data. Furthermore, theoretical considerations on the nature of the heat transfer process rather point to higher heat transfer coefficients compared to the storage of natural gas. From [3] the heat transfer coefficient α can be calculated as:

$$\alpha = 0{,}1\left(\frac{g\beta\rho^2 c_p \lambda^2 (T_w - T_{H_2})}{\nu}\right)^{1/3}$$

with the gravitational constant g, the expansion coefficient β, the density ρ, the specific heat capacity c_p, the heat conductivity λ, the dynamic viscosity ν and the temperature difference between the stored hydrogen and the cavern wall. With realistic values for hydrogen under cavern conditions a heat transfer coefficient in the order of 100 – 200 W/m²/K is obtained.

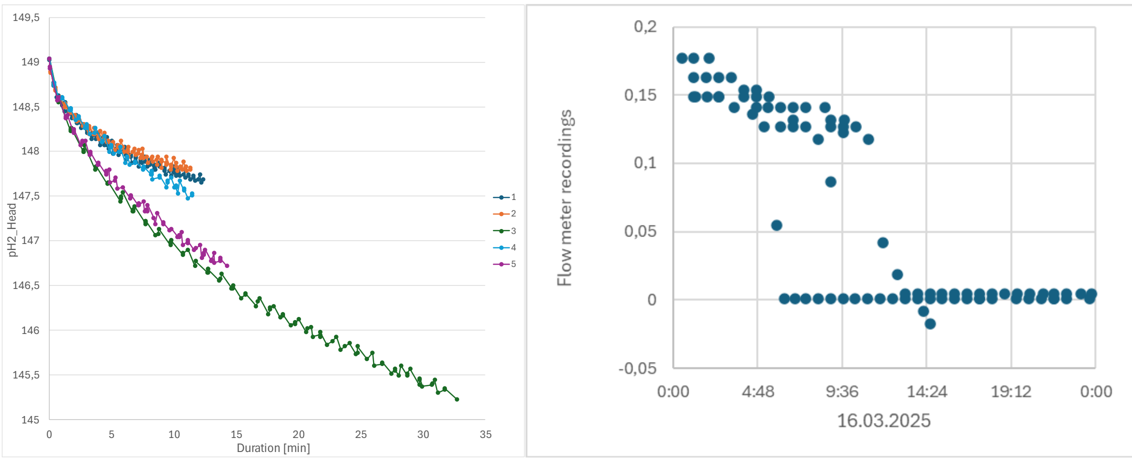

Figure 11: Comparison of hydrogen pressure drop at the wellhead during several standstill periods (left) and flow meter recordings on the 16th of March (right)

Standstill periods at high pressure

The pressure development of the models 1-4 (Figure 8) shows that a stronger thermal coupling leads to a stronger convex curvature of the pressure graphs during the beginning of standstill phases in comparison to the measured pressure development. In particular during the standstill period from 14.03. to 17.03. only Model 4 with a heat transfer coefficient of 1 W/m²/K and without heat transfer to the sump is still decreasing at the end of the standstill period similar to the pressure measurement. However, as derived above, such low heat transfer coefficients are unlikely from a theoretical perspective. Another remarkable feature of the measurements is that during this period, the brine temperature is always significantly higher than the surface temperature indication (see Figure 10), a behavior that would be expected if the brine flow from the cavern has not completely stopped. On the other hand, during other, shorter standstill periods the brine temperature approaches the surface temperature rather quickly.

To better understand this effect the pressure development during several standstill periods is plotted versus the duration of the standstill (Figure 11, left). This shows that the pressure drop is much quicker for the standstill from 14.03. until 17.03. (line 3) and on 04.04. (line 5) compared with the other periods. This behavior would also agree well with a slight continuing brine flow from the cavern in both cases. A following check of the measurement data revealed that indeed the flowmeter has recorded a small brine flow during both periods, that was not considered earlier, because the well was expected to be in shut-in mode. A further detailed analysis of the flow meter recordings showed that only very few values were recorded in the range between 0 and 0.12 (Figure 11, right). As this drop of the flow rate on the 16.03. could not be explained physically, it was assumed that the flow decreases continuously instead of dropping abruptly after passing below 0.12 m^3/h.

Correction of sampling intervals

The length of the sampling periods (granularity of the acquired data) ranges in total from an order of milliseconds to several days, while most have a length of seconds to minutes. Unfortunately, the sampling intervals of the flow meter do not correspond to those of the pressure meter. In several cases, there is only one flow recording while the pressure development shows significant changes. In these cases, the flow sampling intervals have been adjusted to match the pressure sampling intervals.

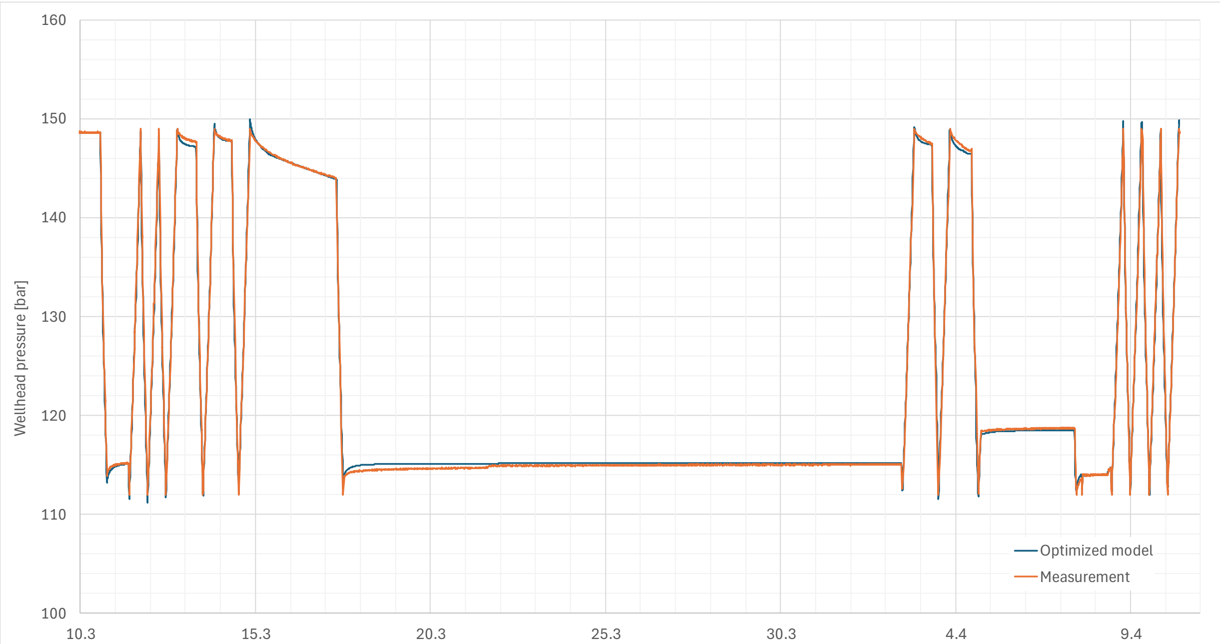

Figure 12: Hydrogen wellhead pressure development of the optimized model

Based on the corrections described above an optimized model was implemented. It comprises a heat transfer coefficient of 150 $W/m^2/K$ and thermal coupling with the cavern sump. Furthermore, the brine level was slightly reduced for 0.5 m (interface level at 929 m at 149 bar) resulting in a slightly larger hydrogen inventory of 2.73 t instead of 2.6 t as estimated from the filling process. Thus, the initial hydrogen volume is 261 m^3 and the sump volume is 7 120 m^3. The resulting pressure development is shown in Figure 12 and the temperature development in Figure 13. The difference of the modeled pressure and the measurement is in the order of less than 1 bar, which is a good value and a significant improvement compared to the initial model. The hydrogen temperature in the cavern is developing in agreement with the pressure development and remains in the range from 39 °C to 49 °C, which is a reasonable range considering the undisturbed rock temperature of 44.6 °C at the depth of the hydrogen-filled cavern center.

Consequently, with the corrections made regarding the recorded flow values and the assumed heat transfer coefficient, this model can be regarded as validated on the test data.

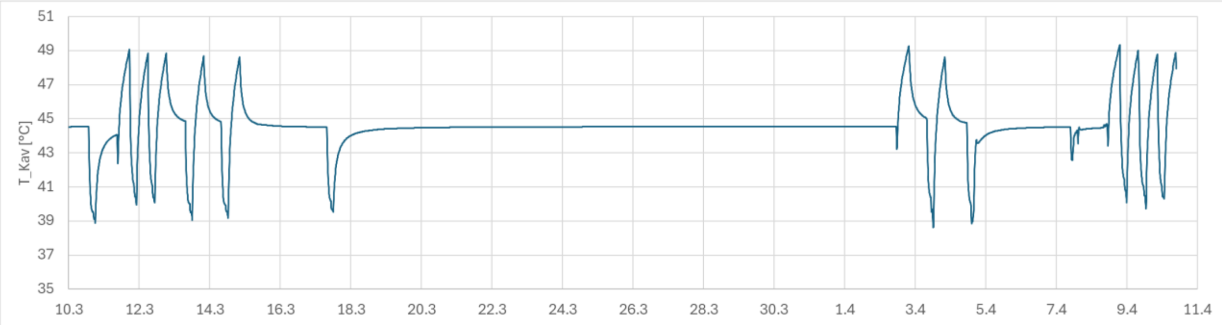

Figure 13: Hydrogen temperature development in the cavern of the optimized model

7. CONCLUSIONS

The experimental campaign conducted within the HyPSTER project has successfully demonstrated the technical feasibility and modeling accuracy of cyclic hydrogen storage in solution-mined salt caverns. The cavern EZ53 served as a representative test site, where controlled brine injection and withdrawal cycles enabled precise manipulation of hydrogen pressure under realistic subsurface conditions.

The thermodynamic modeling framework, primarily based on the KAVPOOL software suite, was rigorously validated against field data, showing strong agreement in pressure evolution across a range of thermal boundary conditions. Notably, the inclusion of thermal coupling effects—particularly between the stored hydrogen and the brine-filled sump—proved essential for reproducing observed system behavior. The validated model now provides a robust tool for simulating hydrogen storage operations and can be confidently applied to industrial-scale scenarios. These findings contribute significantly to the development of reliable, scalable underground hydrogen storage solutions and support the broader integration of hydrogen into Europe’s future energy infrastructure.

For the setup and conduction of further tests the following conclusions can be drawn based on the evaluation process:

- Ensure regular sampling intervals for all measurements, ideally identical intervals for the different quantities (pressure, temperature, flow/balance)
- Measure the balance for all media involved in the testing including brine and additional freshwater (not just rates, which are only momentary values; balances are usually more reliable)
- Install a downhole temperature measurement system, as this can significantly increase the accuracy of the model optimization. Ideally, such system would also allow spatially resolved temperature measurement along the wellbore (like fiber-optical systems).

8. REFERENCES

[1] Hugout, J. (1984). *Outflow and tightness tests on cavern EZ53*. Internal report, Storengy, France..

[2] Brouard, B. (1998). *Brine outflow and leak tests on cavern EZ53*.

[3] Kreith, F. & Black, W. C. (1980). *Basic Heat Transfer*, Harper & Row Publishers Inc., New York

9. ANNEX A – ELECTRONIC FILLING IDENTIFER

Document Name and version	<Model qualification of test caverns on field test data (Deliverable D2.6, final version)>
Description	< This document describes the predictive modeling of the planned EZ53 cyclic test and the modeling of the cyclic test, as it was carried out from December 2024 until April 2025. It concludes with the qualification of the developed model and the applied tools for further industrial application.>
Location	<Project sharepoint\Deliverables>
Filing date	<12/09/2025>

- ACKNOWLEDGEMENT -

This project has received funding from the Fuel Cells and Hydrogen 2 Joint Undertaking (now Clean Hydrogen Partnership) under Grant Agreement No 101006751. This Joint Undertaking receives support from the European Union's Horizon 2020 Research and Innovation programme, Hydrogen Europe and Hydrogen Europe Research.

Co-funded by the European Union

Clean Hydrogen Partnership

The HyPSTER project is co-funded by a consortium of public and private organisations.